An Investigation of the Selenium Concentration in Thenardite Efflorescences on Mancos Shale, Western Colorado

Final Report

Prepared for

Ruth Powell Hutchins Water Center
Colorado Mesa University

Rachael C. Lohse & William C. Hood
Department of Physical and Environmental Sciences
Colorado Mesa University
May 24, 2018

Accomplishments

This is the final report on the accomplishments of the grant "An Investigation of the Selenium Concentration in Thenardite Efflorescences on Mancos Shale, Western Colorado." The major accomplishments were:

We collected 106 samples of the white efflorescences that occur scattered about on the Mancos Shale in Mesa, Delta and Montrose Counties, western Colorado.

In the laboratory, a portion of each sample was purified to remove clays and other particulate impurities. The purified material was pressed into pellets and analyzed for selenium by x-ray fluorescence.

Seven samples were sent to a certified laboratory to give us standards with which to analyze the remaining samples by x-ray fluorescence. Upon establishing a relationship between the x-ray response and selenium concentration, the selenium concentrations in the remaining samples were calculated.

Selenium in the efflorescences ranged from less than one part per million to 441 ppm (by weight).

Experiments were conducted to see if the selenium in the easily soluble efflorescences could be incorporated into gypsum, which is much less soluble. Some selenium was trapped, but most was not, suggesting that the selenium in the efflorescences is not in the form of selenate $(SeO_4)^{-2}$.

Portions of the original material from each of the 106 samples were analyzed by x-ray diffraction to determine the mineralogy. By far the most abundant mineral was thenardite (Na2SO4) although minor amounts of gypsum ($CaSO_4 \cdot 2H_2O$) and bloedite ($Na_2Mg(SO_4)_2 \cdot 4H_2O$) also occur. Bloedite was the major phase in one sample.

The results of the project were presented by Rachael at the CMU Student Showcase and then again to the Grand Junction Geological Society at their April, 2017 meeting. Rachael won a small cash award for her poster at the GJGS meeting.

An abstract of the work was submitted to the Rocky Mountain Section of the Geological Society of America for consideration for presentation at their May meeting. The abstract was accepted and is published on the GSA website (Lohse and Hood, 2018).

We presented a slightly revised version of the poster at the RMS-GSA meeting in Flagstaff, AZ, on May 15, 2017. A photograph of the poster and authors is below (Fig. 1).

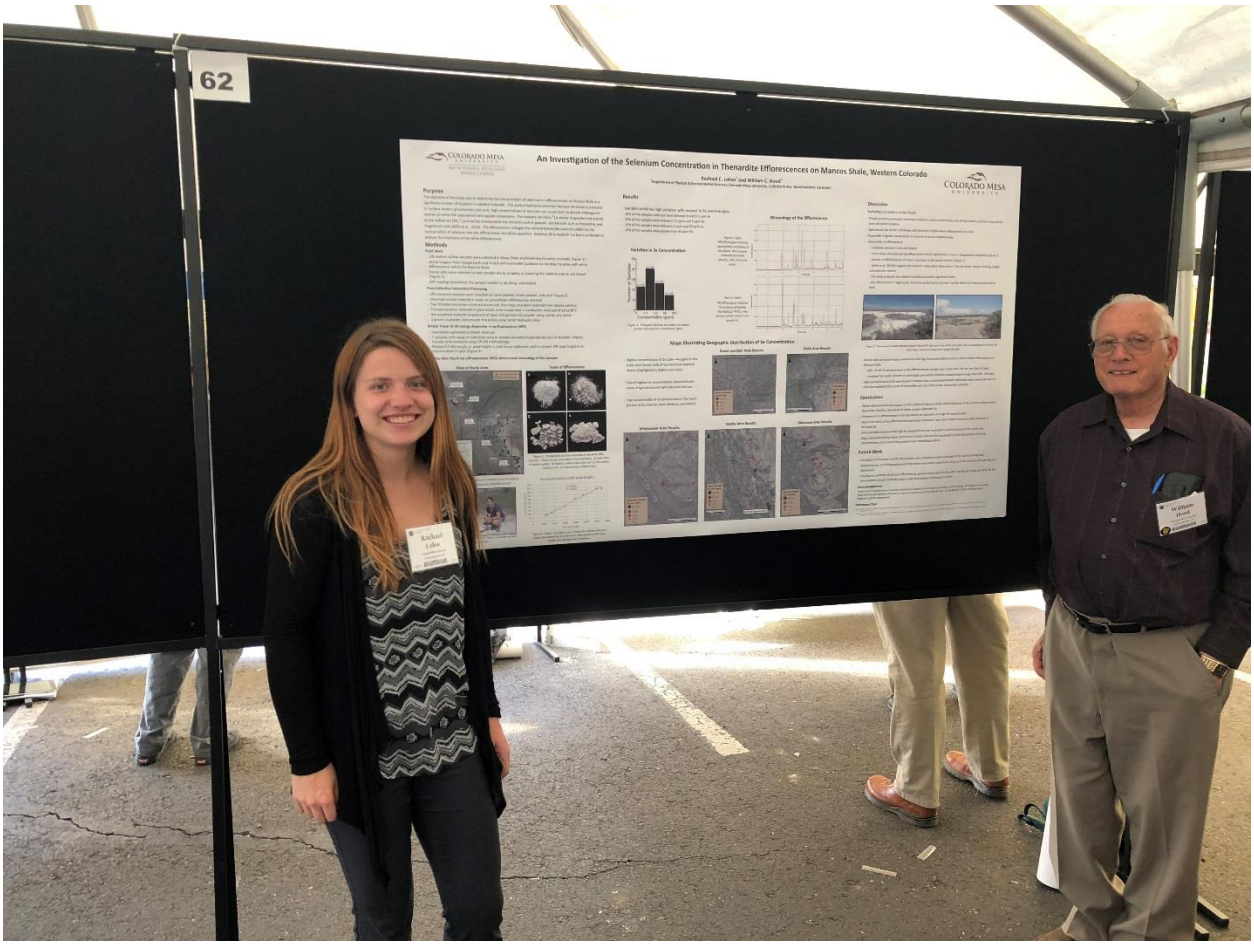

Figure 1. Rachael Lohse and William Hood with their poster at the RMS-GSA meeting in Flagstaff, AZ on May 15, 2018.

Introduction

The presence of selenium in rocks, including rock units that are equivalent to the Mancos Shale, has been known for decades (Howard, 1969a,b; Rapp and Patraw, 1966). In 1982, when the mortality of fish and birds and the lowered reproductive success for birds in the Kesterson Wildlife Refuge in California was traced to selenium in water (National Research Council Committee, 1989). The source of the selenium was then traced to irrigation. This led to other studies that identified selenium problems in the Green River drainage in Utah (Stephens et al., 1988) and in the Colorado and Gunnison Basins in western Colorado in 1987-1988 (Butler, et al., 1996). It was established that irrigation was contributing much of the selenium load to the water of the western Colorado area (Wright and Butler, 1993) and work subsequently has concentrated on ways to reduce the selenium load. Experimental projects involving bioremediation (Walker and Golder Associates, 2010) and phytoremediation (Fisher, 2005) have been conducted and much effort has gone into controlling underground seepage from irrigation structures (Butler, 2001). Recent investigations have examined the presence of selenium in weathered Mancos Shale (Tuttle et al., 2014a, b) and in unweathered Mancos Shale in deep drill holes (Hood and Cole, 2016).

This study emphasizes selenium because the metal is prevalent in western Colorado surface waters, groundwater, and soils. Although small amounts of selenium are necessary for health in both animals and man, high concentrations of selenium can cause harm to already endangered species of native fish populations and aquatic ecosystems. Extreme selenium toxicity cases can cause death to farm animals, wildlife and even man (Koller and Exon, 1986). We observed many instances of selenium accumulator plants such as *Stanleya pinnata* (Princes Plume) and species *Astragalus* growing in the vicinity of the efflorescences. However, the plant most commonly observed in the efflorescences themselves was *Hallogeton glomeratus*, a salt-tolerant, oxalate-accumulating plant that can be toxic to sheep (James and Cronin, 1974).

Selenium is naturally sourced from the Mancos Shale which covers significant portions of western Colorado. The shale weathers easily and thus provides an optimal pathway for selenium to enter the waters. As the shale weathers, the reduced forms of selenium in selenopyrite or organic matter can be oxidized and released into solution (Mills et al., 2016). It is most commonly leached by means of agricultural and domestic irrigation and leakage from irrigation canals (Butler et al., 1996). In many places a white efflorescence occurs where seepage from natural springs and seeps, irrigation ditches and canals reaches the surface and evaporates. The efflorescence, commonly called "alkali" by local residents, is very high in sodium and makes plant growth difficult. The springs and seeps in the area often contain high quantities of selenium (Morrison et al., 2012). It seems probable that if ground and surface waters contain excessive amounts of selenium, then the efflorescences derived from seepage of ground water ought to contain selenium as well.

The main objective of the study was to determine the concentration of selenium in a significant number of locations in western Colorado. The selenate ion is similar in geochemical activity to the sulfate ion and can be incorporated into minerals such as gypsum, soluble salts such as thenardite, and magnesium salts (Mills et al. 2016). Previous work by Hood (unpublished) indicated that the efflorescence is largely the mineral thenardite (sodium sulfate) so the incorporation of selenium into the efflorescence should be expected. However, little research has been conducted to analyze the chemistry of the white efflorescence.

According to Tuttle et al. (2014a), natural undisturbed landscapes contribute only very small amounts of selenium to the waterways of western Colorado. Precipitation from rain or snow dissolves calcium and other ions on the land surface. The solutes percolate into the subsurface to form gypsum and soil moisture containing sodium sulfate. The arid conditions following the moisture event evaporate some of the soil moisture, concentrating the sodium sulfate which is quite soluble. This portion of the state experiences around 9.5 to 10 inches of precipitation annually. This is not enough precipitation to attribute to the large amount of salinity in the rivers currently. Most of the contamination is derived from irrigated soils. Irrigation accelerates the rate at which the sodium sulfate salts and selenate reaches the waterways.

Methods

One-hundred and six sodium sulfate samples were collected in Mesa, Delta and Montrose Counties, Colorado (Table 1 and Figure 2). Aerial imagery from Google Earth and ArcGIS

online provided guidance on locating the white efflorescences within the Mancos Shale. The purest salts were collected at each sample site by scraping or scooping the material with an ash shovel. A GPS reading was recorded at the sample location in lat./long. coordinates with a Garmin eTrex and DeLorme Earthmate PN-60. Elevations of the sample sites were determined by using a DEM (digital elevation model) of western Colorado in ArcGIS. The samples were classified as: pure powder, mixed powder, and crust. Examples are shown in Figure 3.

Samples were processed and analyzed in the advanced geology and x-ray laboratory at Colorado Mesa University following the field collection. The sodium sulfate was concentrated by dissolving the crustal material in water. Soil and plant material were removed by funneling the solution through coffee filters into glass bottles. A second filtration with Whatman No. 42 filter paper removed finer clay particles and ensured the solution consisted of purely dissolved material. The second filtrate was collected in glass bowls that were placed in a convection oven and dried at approximately 90 degrees Celsius. The recrystallized material in the glass bowls was scraped out and ground to a powder by hand using a mortar and pestle. About two grams of the powder was put into a Spex Sample Prep between two 13mm dies. A Carver hydraulic press applied pressure of about 5000 psi to compress each sample into a pellet. The pellets were analyzed for selenium using a Bruker Tracer III-SD energy dispersive x-ray fluorescence (XRF) instrument optimized to detect selenium and elements with x-ray fluorescence characteristics similar to selenium. The instrument produces a graph of photons detected over a period of time vs energy level. The intensity of the selenium peak for each sample was calculated after correction for background noise. Seven samples with a range of selenium peak intensities were sent to Actlabs (Activation Laboratories Ltd.) in Ancaster, Ontario, Canada to be analyzed by ICP-MS methodology. The results from these analyses compared with the corresponding XRF peak intensities yielded a linear calibration plot which then allowed us to convert the selenium peak heights into concentration in ppm (Figure 4).

To determine if the selenium in the efflorescences can be locked up in the mineral gypsum, calcium chloride dihydrate was added to the set of samples with the highest concentration of selenium. Calcium chloride is very soluble, quickly goes into solution and can then react with the dissolved sulfate to form the much-less-soluble mineral, gypsum. The chemical reaction is: Na_2SO_4 (aq.) + $CaCl_2 \cdot 2H_2O$ (s) → $CaSO_4 \cdot 2H_2O$ (s, gypsum) + $2NaCl_2$ (aq.). The liquid and precipitated gypsum were then centrifuged to concentrate the gypsum. The gypsum was separated from the solution and dried. The solution was evaporated to dryness in the oven, producing a product that is mostly salt (NaCl). The gypsum and salt were then pressed into pellets and analyzed for selenium by XRF.

To determine the original mineralogy of the efflorescences, a portion of each sample was sieved to collect the silt and clay fraction. This was done because it was recognized that the efflorescences usually consisted of a fine white powder and so could be concentrated by a size separation. For samples that consisted of a hard crust, we simply broke off a piece of crust and pulverized it. The powders contained the efflorescence material plus quartz, clay and other impurities. A portion of each powder was placed into a sample holder and the minerals identified by x-ray diffraction.

Results

The results of the selenium analyses of the efflorescences are presented in Table 2 and are summarized here. Twenty percent of the samples collected were between zero and 0.5 ppm. Thirty-nine percent of the samples were between 0.5 ppm and 5 ppm. Twenty-five percent of the samples were between 5 ppm and 50 ppm and fourteen percent were greater than 50 ppm (Figure 5). The maximum concentration found was 441 ppm in sample WP36. Maps showing the sampling locations and the analytical results are shown in in Figures 6 – 10). Larger symbols represent higher concentrations while small symbols represent lower concentrations. Low concentrations were prevalent in the southernmost portion of the Montrose samples and graduate to moderate/larger concentrations northward. The highest concentrations of selenium found in the study were just north of the Montrose Regional Airport. This is highlighted in the Olathe area result map. The land use in this area consists of agricultural and commercial development. The Delta area contained two high concentrated samples in the center of the town in an area surrounded by commercial development. The samples in the surrounding area recorded low to moderate concentrations. Whitewater contained two localized 'hot spots' east of Highway 50 where concentrations were greater than 100 ppm. A small number of samples were collected in Grand Junction. The highest Se values were within the city limits surrounded by commercial development.

With regard to the gypsum precipitation experiment, the selenium concentrations in the gypsum precipitate were compared selenium concentrations in the salt, which represents the selenium not incorporated in the gypsum. Overall, the Se concentrations the gypsum precipitates averaged 17 ppm whereas the concentration in the salt residue averaged 80 ppm.

Results of the mineralogy investigation are presented in Table 3. As expected from the previous work by Hood (unpublished research) and the examination of 16 samples of the purified efflorescence, the predominant mineral in the efflorescence samples is thenardite (sodium sulfate – Na_2SO_4). Small amounts of gypsum ($CaSO_4.2H_2O$) and bloedite ($Na_2Mg(SO_4)_2.4H_2O$) were found in several samples. Because the samples also contained quartz, clay minerals, calcite and possibly other minerals, the x-ray diffraction patterns were difficult to interpret. We used a XRD interpretation program, PDXL, supplied by the manufacturer of our instrument, to assist in the interpretation. This program is adept at identifying single minerals but does not do a very good job at identifying minerals in mixtures, especially when more than two minerals are present. We had to resort to a very time-consuming procedure of eliminating the peaks for quartz and thenardite and then trying to identify any other minerals that might be present based on the remaining diffraction peaks. Small amounts of other sulfate minerals (mirabilite, hexahydrate, vanthoffite, and leowite) were possibly present but could not be identified with certainty. Because the Mancos Shale is a marine deposit, we made a specific search for diffraction peaks related to the mineral halite (sodium chloride) but were unable to find any evidence that the mineral is present.

Discussion

There were several limitations involved with the sample collection. Private property prevented collecting samples in some circumstances. Verbal permission was granted in many cases; however, land owners were unable to be contacted for some desirable locations. Agricultural land use also posed a challenge to collecting samples, with livestock in the fields where the efflorescence occurred. Impassible irrigation canals acted as a barrier to access to some areas, including some with large amounts of efflorescence. The seasonality of the efflorescence also limited the sample collection. We collected samples in July and August. During the summer months, many of the areas characterized by efflorescence had shrunk significantly in size or disappeared entirely. The patches of efflorescence will return and grow in the winter months (Figure 11). Tuttle et al. (2014b) suggest that moisture evaporation takes place in the dry winter months forming sulfate and selenate mineral. While this is true, it is not the entire story. Grand Junction receives an average of 9.4 inches of precipitation per year, with the highest amounts in September and October (about 1.2 inches) and the lowest in June (0.47 inches). February is also low. The city of Montrose is similar, with an average annual precipitation of 10.19 inches (www.usaclimatedata.com). The significant factor is relative humidity. In the winter months, relative humidity reaches a daily average of 70% in January. It falls steadily down to 29% in June and stays below 40% through September (www.currentresults.com/weather/). Many days during June, July and August the relative humidity in the afternoons falls below 10% (personal observation). We hypothesize that the efflorescences are slightly hydroscopic and when the humidity is high the particles tend to stick together. During the hot, dry summer days with low humidity, they lose moisture and tend to get blown away by the wind, except in areas where significant seepage keeps them moist.

The analytical results did not reveal a strong relationship between high selenium concentration and sodium sulfate efflorescences in the Mancos Shale as originally hypothesized. Many of the selenium concentrations are fairly low, less than one part per million. However, there are localized 'hot spots' in each study area where selenium concentrations range from 100 to over 400 ppm. It was determined with the GIS data that the locations with the highest concentrations are not in depressions or in areas characterized by low elevations. This shows selenium concentrations have no apparent relationship with topography. The highest selenium concentrations were not in the purest thenardite collected as we had hypothesized before beginning the project. They were mainly in samples that contained powdered thenardite salts mixed with soils or soils that exhibited thin crusts of thenardite.

The experiment that was conducted in an attempt to contain the selenium present in the sodium sulfate by precipitating gypsum was partly successful. Although some of the selenium was immobilized in gypsum, the results indicated that the selenium predominantly stayed in the solution rather than being precipitated with the gypsum. The selenate ion (SeO_4^{-2}) and sulfate (SO_4^{-2}) are similar in size, structure and charge, which allows the selenate ion to be incorporated into gypsum. The fact that selenium stayed in solution indicates the majority of selenium within the samples is in a form other than the selenate ion. Alternatives include the other three oxidation states of selenium: selenite (SeO_3^{-2}), selenide (Se^{-2}), and elemental Se. Selenide and elemental Se are the least abundant in the Mancos Shale (Tuttle et al. 2014a). Therefore, we

hypothesize that selenite is likely present because dissolved selenium primarily exists as selenite or selenate in the Mancos shale depending on redox conditions (Mills et al. 2016). Immobile phases, especially adsorbed selenite (SeO_3^{-2}), happen to make up most of the selenium in Mancos Shale soil (Tuttle et al. 2014a). Selenite (SeO_3^{-2}) is known to absorb into clays, hydrous ferric oxides, or organic matter (Mills et al. 2016). We are currently unable to verify if all the selenate (SeO_4^{-2}) entered the gypsum.

The mineralogy investigation confirmed that the main mineral component of the efflorescences is thenardite (sodium sulfate). The total absence of any chloride mineral in the efflorescences indicates that the sodium did not originate as trapped amounts of ancient sea water. It must be present as part of the clay minerals in the shale, either as interlayer cations or as exchange cations on clay surfaces. The sulfate in the efflorescences most probably comes from the oxidation of pyrite (iron sulfide), which produces sulfuric acid as one of the products. We suggest that the hydronium ion from the acid attacks the clay minerals in the shale, releasing sodium in the process. Small amounts of magnesium are also released to give rise to the bloedite.

Conclusions

White efflorescences that appear on the surface of Mancos Shale consist primarily of the sodium sulfate mineral, thenardite, almost all of which contain detectible selenium. However, the presence of an efflorescence is not necessarily an indication of a high selenium concentration. About one-third of the efflorescences examined contained 1 ppm selenium or lower but some contained as much as 441 ppm selenium. However, the study provides evidence that high selenium concentrations are confined to certain locations in the study area. The maps with graduated symbols produced in ArcGIS enhance the visualization of the distribution of the selenium concentrations and should help guide future remediation efforts. The experiment revealed that the selenium phases in the shale are likely in the forms of selenate (SeO_4^{-2}) and selenite (SeO_3^{-2}).

Acknowledgements

We thank Colorado Mesa University's Ruth Powell Hutchins Water Center for providing financial support for this project. Sandra Hood helped with sample collection as well as transporting us to and from the field sites. Colorado Mesa University chemistry department provided the calcium chloride for the gypsum precipitation experiments.

References Cited

Butler, D.L., 2001, Effects of Piping Irrigation Laterals on Selenium and Salt Loads, Montrose Arroyo Basin, Western Colorado: U.S. Geological Survey Water-Resources Investigations Report 01–4204, 14 p.

Butler, D.L., Wright, W.G., Stewart, K.C., Osmundson, B.C., Krueger, R.P., and Crabtree, D.W., 1996, Detailed study of selenium and other constituents in water, bottom sediment, soil, alfalfa, and biota associated with irrigation drainage in the Uncompahgre Project Area and in the Grand Valley, west-central Colorado, 1991-93: U.S. G. S. Water Resources Investigations Report 96-4138, 136 p.

Fisher, F.S., 2005, Uncompahgre Basin selenium phytoremediation: U.S. E.P.A. Grant WQC 01-00057 Final Report, 150 p.

Hood, W. C. and R. D. Cole (2016) Geochemistry of the Mancos Shale as shown by the Fees Federal 2-6-8-101 well. Search and Discovery, Article 51357, 4 p.

Howard, J.H., 1969a, Geochemistry of selenium in earth-surface environments: *in* Abstracts for 1968: Geol. Soc. America Spec. Paper 121, p. 446.

Howard, J.H., 1969b, Selenium in the Upper Cretaceous Niobrara Formation and Pierre Shale of south-central Colorado, in Abstracts for 1968: Geol. Soc. America Spec. Paper 121, p. 606.

James, L. F., and Cronin, E. H., 1974, Management practices go limit death losses of sheep grazing on *Halogeton*-infested range: Jour. Range Manage., 27, p. 424-426.

Koller, L. D. and Exon, J. H., 1986, The two faces of selenium – deficiency and toxicity – are similar in animals and man: Can. Rev. Vet. Res., v. 50, 297-306.

Lohse, R. C.. and Hood, W. C., 2018, An investigation of the selenium concentration in thenardite efflorescences on Mancos Shale, western Colorado: Geological Society of America Abstracts with Programs. Vol. 50, No. 5, ISSN 0016-7592, doi: 10.1130/abs/2018RM-313456.

Mills, T.J., Mast, M.A, Thomas, J., & Keith, G., 2016, Controls on selenium distribution and mobilization in an irrigated shallow groundwater system underlain by Mancos Shale, Uncompahgre River Basin, Colorado, USA: Science of the Total Environment, v. 566-567, p. 1621-1631.

Morrison, S. J., Goodknight, C. S., Tigar, A. D., bush, R. P., and Gil, A., 2012, Naturally occurring contamination in the Mancos Shale: Environ. Sci. and Technology, 46, p. 1379-1387

National Research Council Committee on Irrigation-Induced Water Quality Problems, 1989, Irrigation-Induced Water Quality Problems. National Academy Press, 157 p.

Rapp, G. R., and Patraw, J.A., 1966, Distribution of selenium in the Niobrara Formation of the Black Hills region, South Dakota (abstract); Geological Society of America Special Paper 87, p. 300.

Stephens, D.W., Waddell, B., and Miller, J., 1988, Reconnaissance investigation of water quality, bottom sediment, and biota associated with irrigation drainage in the middle Green River Basin, Utah, 1986-87: U.S. Geological Survey, Water Resources Investigations Report 88-401.

Tuttle, M. W., Fahy, J. W., Elliott, J. G., Grauch, R. I., & Stillings, L. L. (2014a) Contaminants from Cretaceous Black Shale; I, Natural Weathering Processes Controlling Contaminant Cycling in Mancos Shale, Southwestern United States, with Emphasis on Salinity and Selenium: Applied Geochemistry, Vol. 46, 01 July 2014, p. 57-71.

Tuttle, M. W., Fahy, J. W., Elliott, J. G., Grauch, R. I., & Stillings, L. L. (2014b) Contaminants from Cretaceous Black Shale; II, Effect of Geology, Weathering, Climate, and Land Use on Salinity and Selenium Cycling, Mancos Shale Landscapes, Southwestern United States: Applied Geochemistry, Vol. 46, p. 72-84.

Walker, R., and Golder Associates, Inc., 2010, Passive selenium bioreactor – pilot scale testing: U.S. Bureau of Reclamation Science and Technology Program, Project 4414 Final Report.

Wright, W. G., and Butler, D.L., 1993, Distribution and mobilization of dissolved selenium in ground water of the irrigated Grand and Uncompahgre Valleys, Western Colorado, *in* Allen, R.G., *ed*., Management of irrigation and drainage systems: integrated perspectives: American Society of Civil Engineers, Reston, VA, v. 1024, p. 770-777.

Figure 2

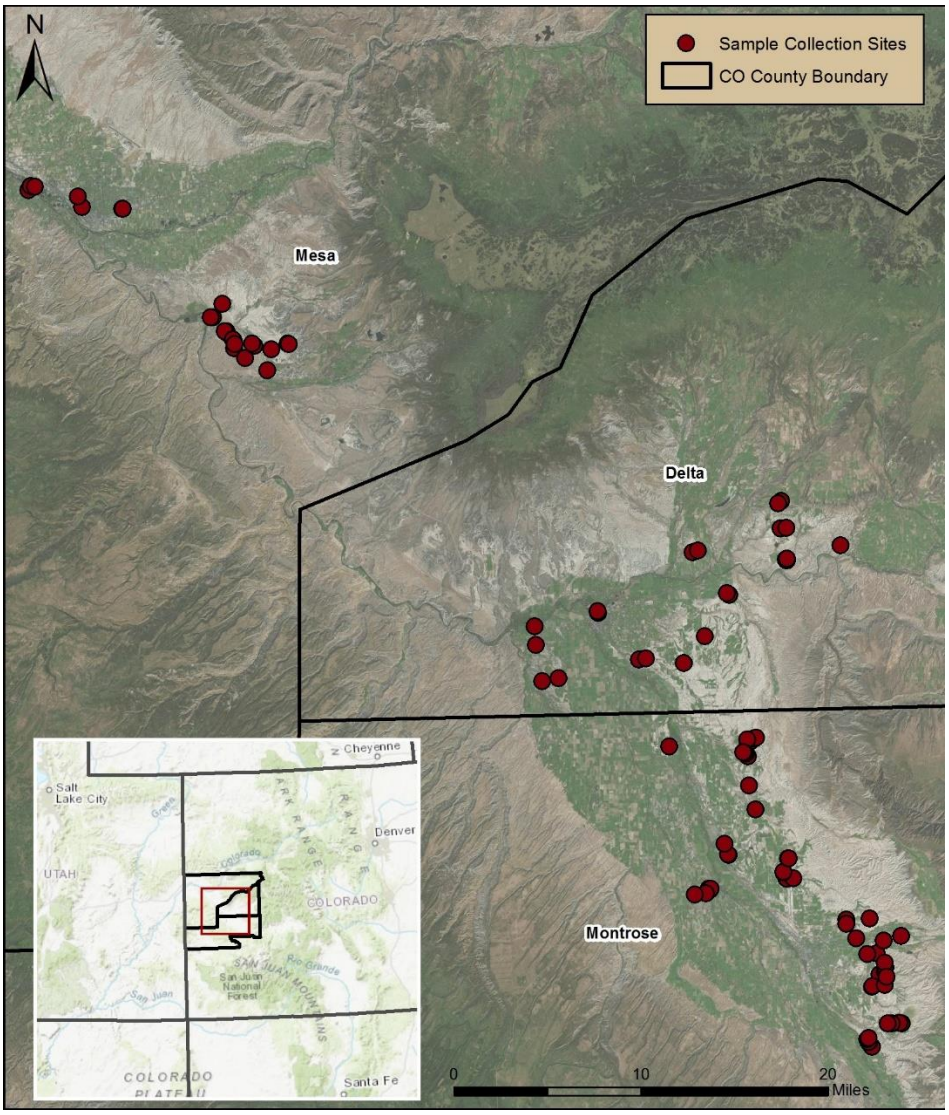

Figure 2. Map showing the locations of collection sites throughout western Colorado (imagery courtesy of ArcGIS online).

Figure 3

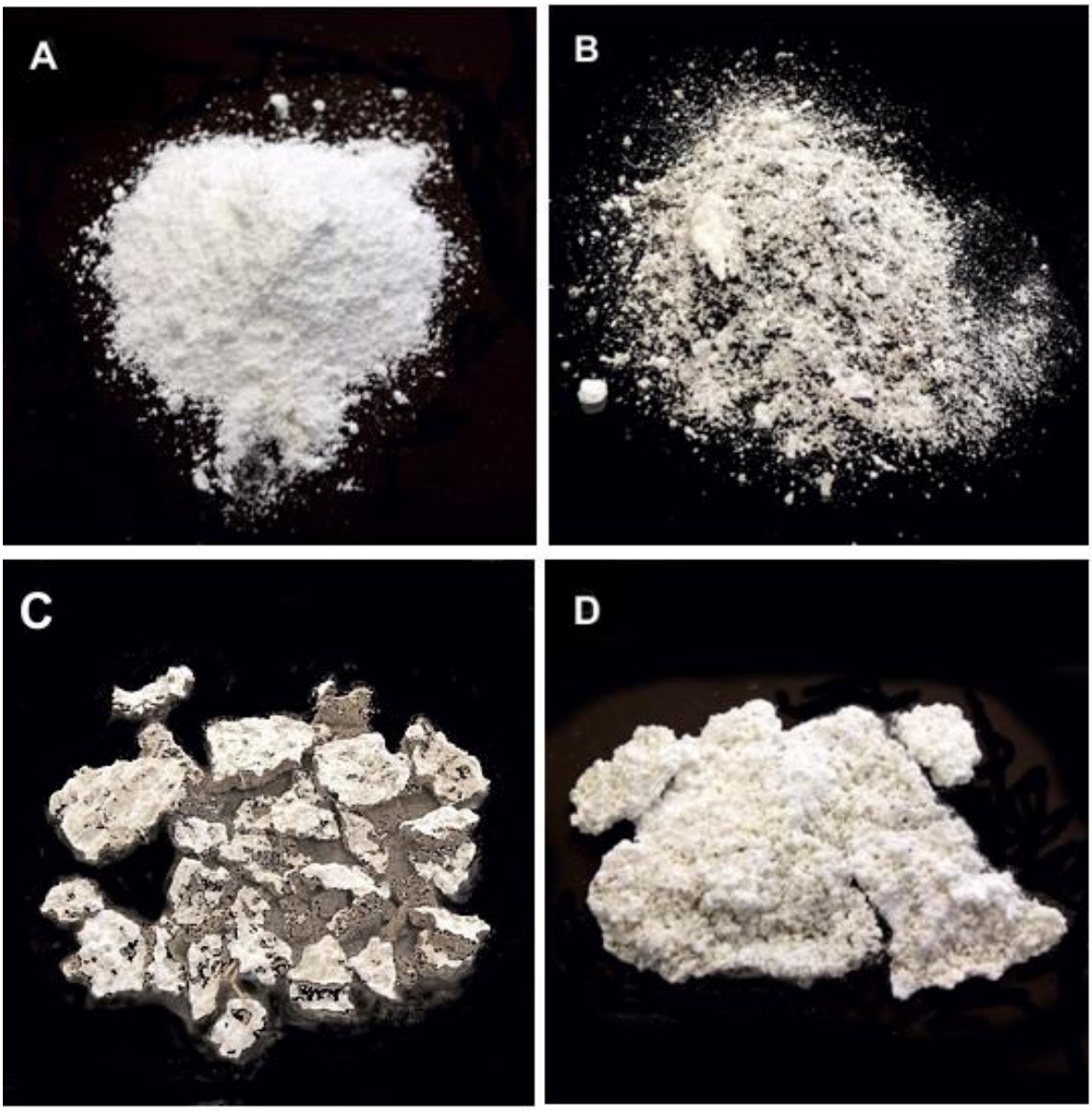

Figure 3. Photographs of some examples of the white efflorescence. These photos were taken in the laboratory. A. Purer form of sodium sulfate. B. Sodium sulfate mixed with soil. C. Thin sulfate crusts on soil. D. Thick sodium sulfate crusts.

Figure 4

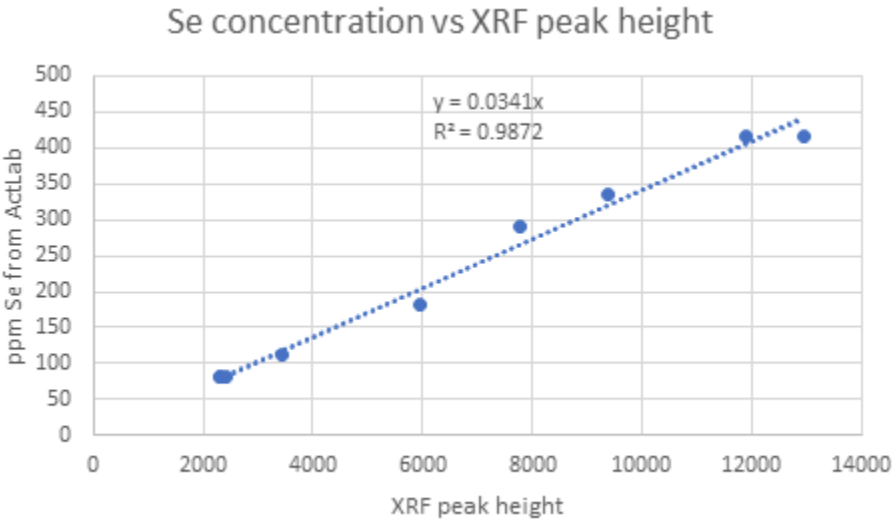

Figure 4. Calibration curve created by relating selenium values determined by ICP-OES at ACT Labs plotted to XRF peak height after background correction.

Figure 5

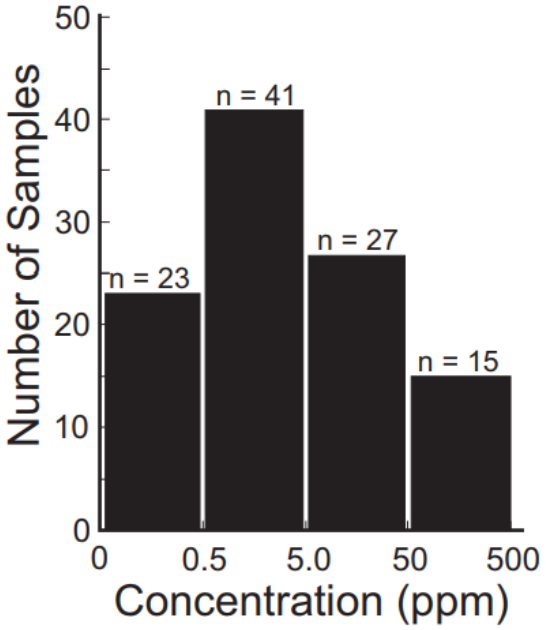

Figure 5. Histogram showing the number of samples plotted with selenium concentration (ppm).

Figure 6

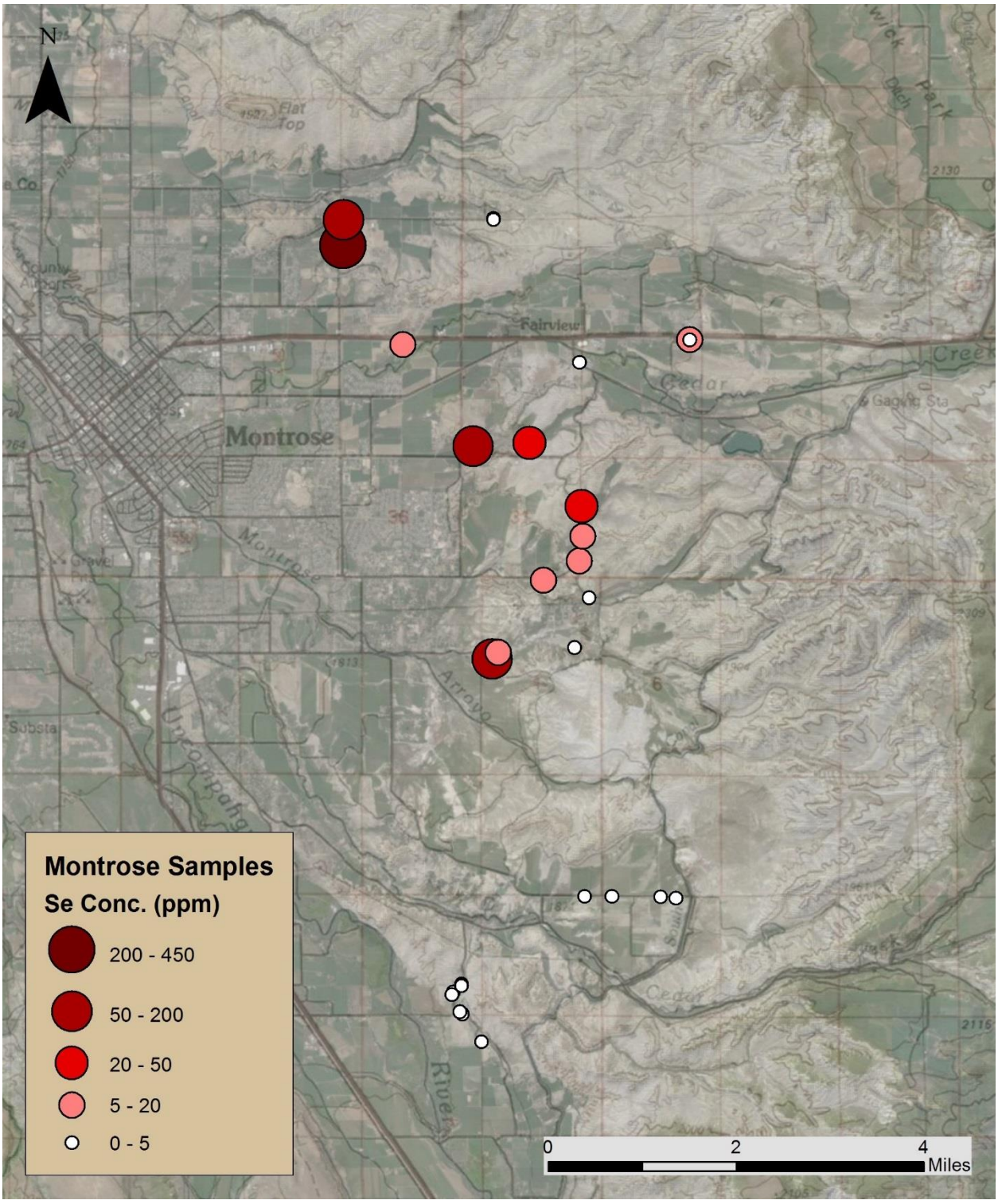

Figure 6. Selenium concentrations (ppm) in efflorescences collected in the Montrose, Colorado area (imagery courtesy of ArcGIS online).

Figure 7

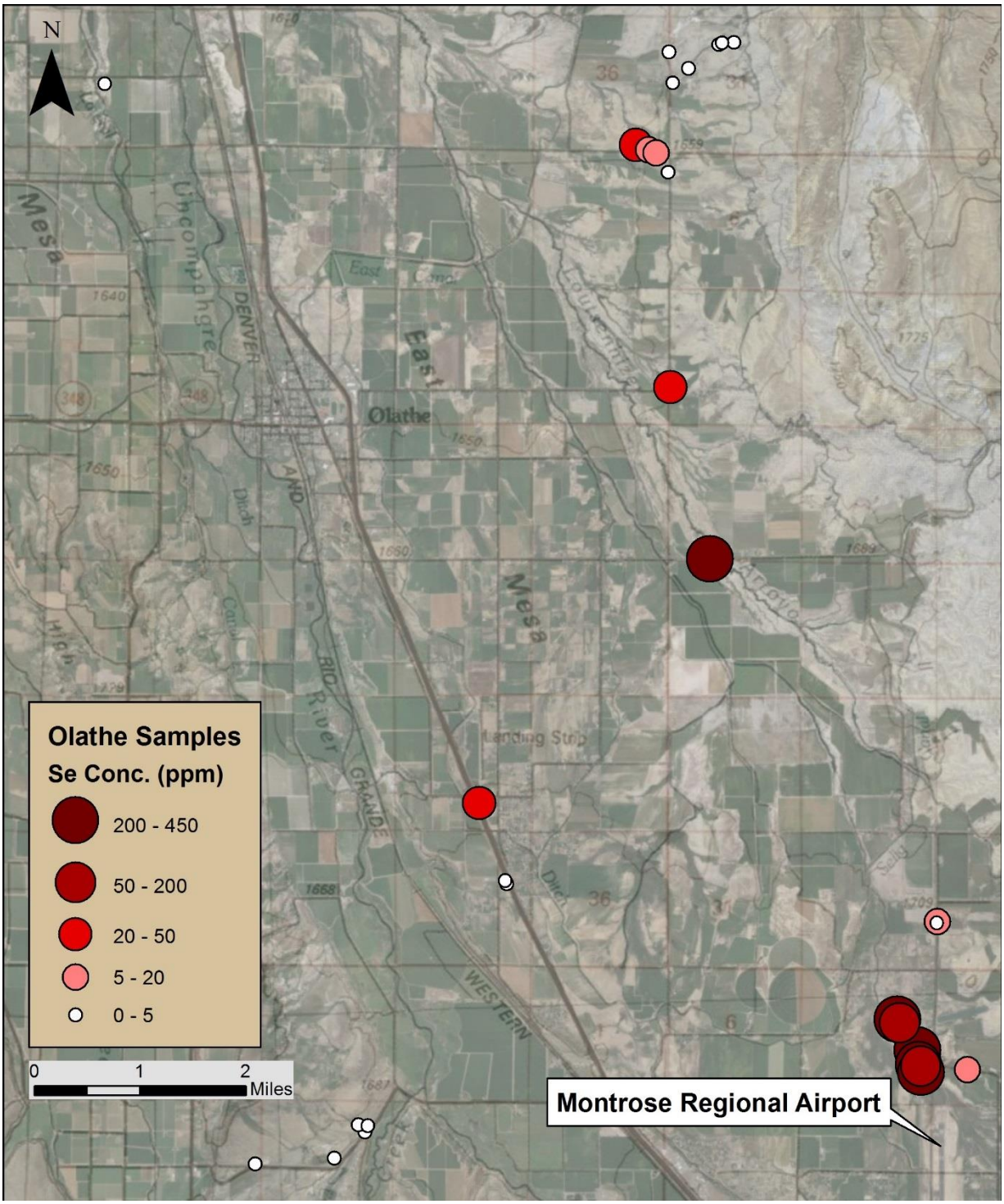

Figure 7. Selenium concentrations (ppm) in efflorescences in the vicinity of Olathe, Colorado (imagery courtesy of ArcGIS online).

Figure 8

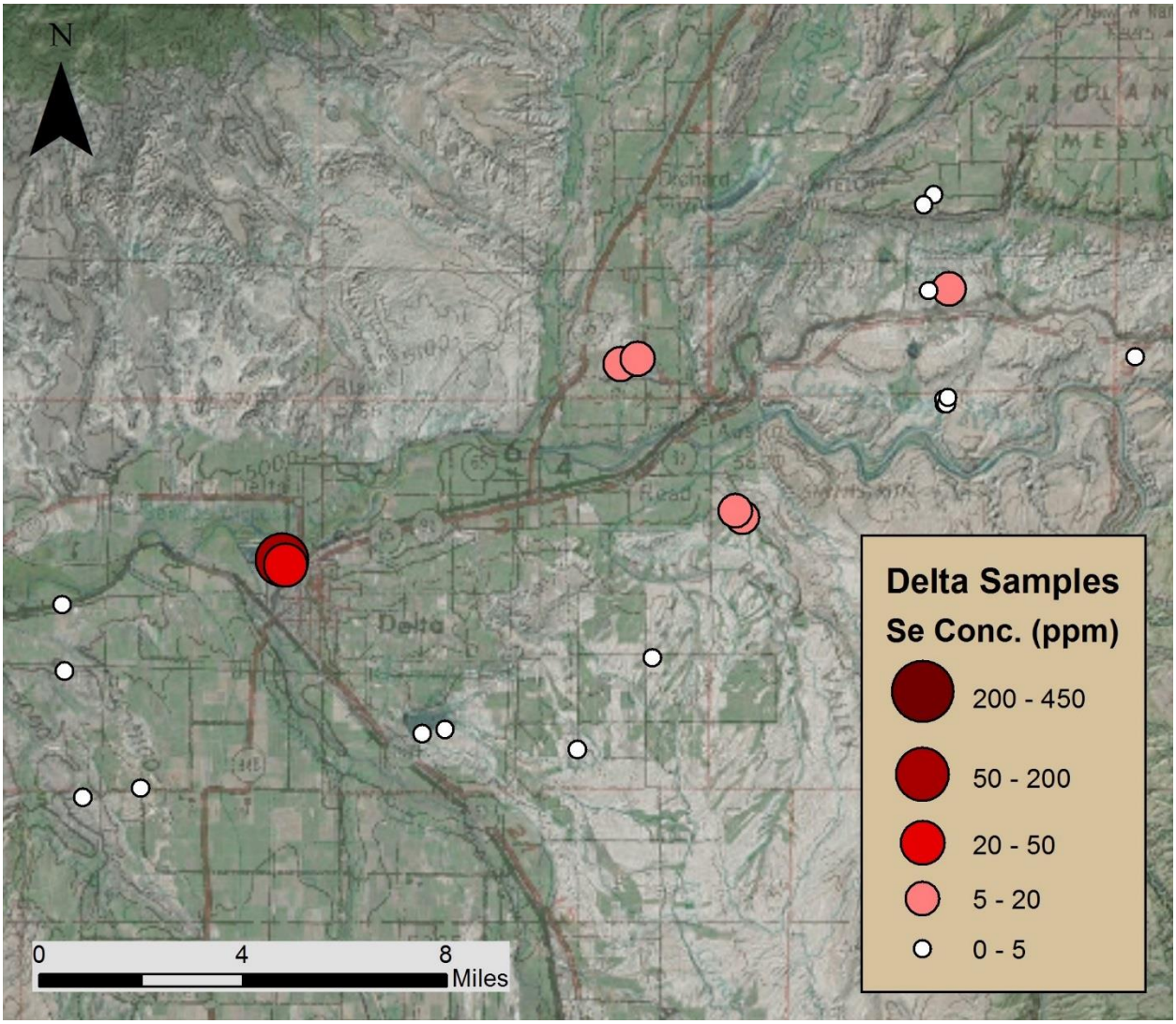

Figure 8. Selenium concentrations (ppm) in efflorescences collected in the vicinity of Delta, Colorado (imagery courtesy of ArcGIS online).

Figure 9.

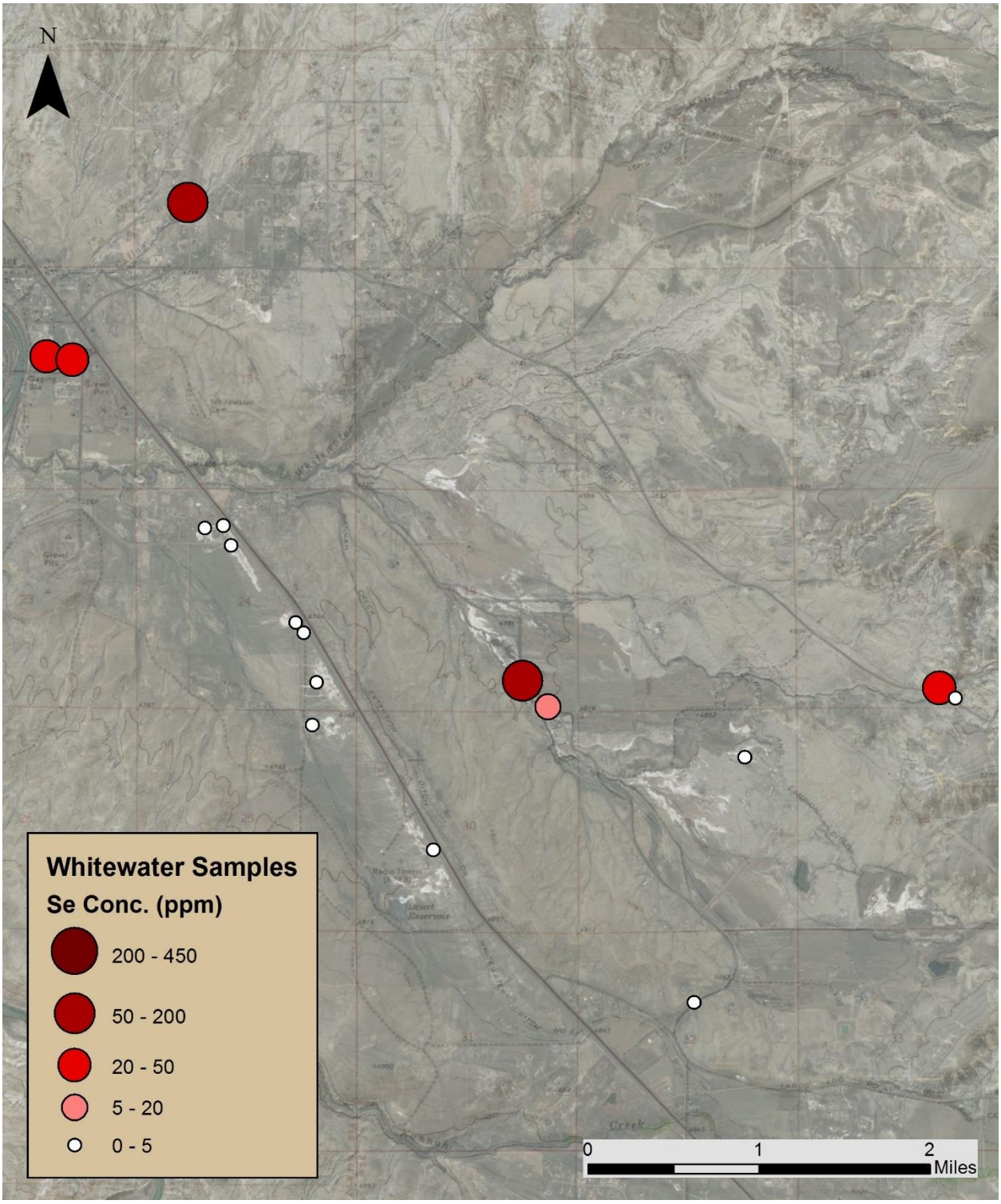

Figure 9. Selenium concentrations (ppm) in efflorescences collected in the Whitewater, Colorado area. (imagery courtesy of ArcGIS online).

Figure 10.

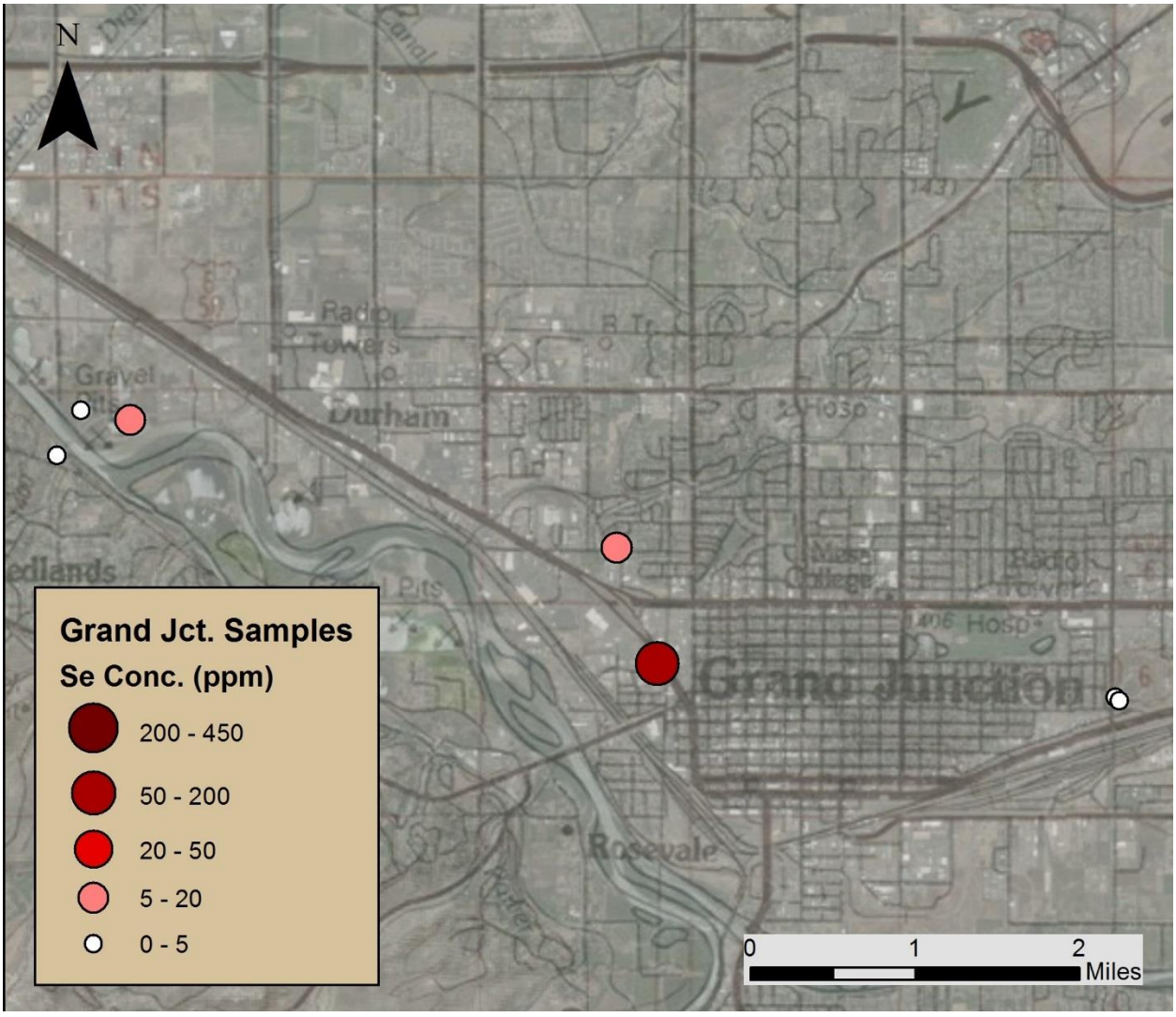

Figure 10. Selenium concentrations (ppm) in efflorescences collected in the Grand Junction, Colorado area. (imagery courtesy of ArcGIS online).

Figure 11.

Figure 11. Two views of sample collection area SP 102 and SP 106 taken close to the same spot. Top: First sampling trip in March (SP 102). Bottom: Second sampling trip in August (SP 106).

Table 1. Locations of the samples used in this study.

Sample	Latitude	Longitude	Sample	Latitude	Longitude	Sample	Latitude	Longitu
1	38.48814	-107.82924	**45**	38.56480	-107.95604	**89**	38.94237	-108.393
2	38.50319	-107.81528	**46**	38.63224	-107.93019	**90**	38.60928	-107.929
3	38.50334	-107.81528	**47**	38.64179	-107.92948	**91**	38.59090	-107.924
4	38.50319	-107.83844	**48**	38.64335	-107.92739	**92**	38.55214	-107.893
5	38.50009	-107.83846	**49**	38.64585	-107.92323	**93**	38.70957	-108.034
6	38.47626	-107.80972	**50**	38.64605	-107.92276	**94**	38.71056	-108.027
7	38.47592	-107.81844	**51**	38.64611	-107.92114	**95**	38.98460	-108.446
8	38.45972	-107.80762	**52**	38.64510	-107.93006	**96**	38.98481	-108.448
9	38.46205	-107.80208	**53**	38.63431	-107.93179	**97**	38.99489	-108.436
10	38.46500	-107.80149	**54**	38.63467	-107.93284	**98**	38.96304	-108.373
11	38.46867	-108.80174	**55**	38.63518	-107.93457	**99**	38.96237	-108.371
12	38.48597	-107.80206	**56**	38.64168	-108.00726	**100**	39.07314	-108.573
13	38.42138	-107.78721	**57**	38.69542	-108.13078	**101**	39.08105	-108.577
14	38.42154	-107.78951	**58**	38.69745	-108.11430	**102**	39.07089	-108.533
15	38.42157	-107.79704	**59**	38.70608	-107.99005	**103**	39.08733	-108.626
16	38.42160	-107.80125	**60**	38.72630	-107.96880	**104**	39.09041	-108.624
17	38.45022	-107.81545	**61**	38.75752	-107.94306	**105**	39.08975	-108.619
18	38.45104	-107.81462	**62**	38.75893	-107.94500	**106**	39.07065	-108.533
19	38.48871	-107.78506	**63**	38.73810	-108.13667			
20	38.40407	-107.81713	**64**	38.72348	-108.13610			
21	38.40743	-107.82010	**65**	38.79154	-107.97776			
22	38.40771	-107.82050	**66**	38.79275	-107.97288			
23	38.41005	-107.82153	**67**	38.80784	-107.89010			
24	38.40973	-107.82169	**68**	38.80818	-107.88420			
25	38.41102	-107.82022	**69**	38.82910	-107.88867			
26	38.41083	-107.82023	**70**	38.82697	-107.89150			
27	38.41031	-107.82075	**71**	38.78262	-107.88503			
28	38.45160	-107.80280	**72**	38.78263	-107.88558			
29	38.45761	-107.80057	**73**	38.78371	-107.88583			
30	38.53841	-107.89604	**74**	38.78411	-107.88469			
31	38.53684	-107.89583	**75**	38.79317	-107.83131			
32	38.53670	-107.89557	**76**	38.74698	-108.07311			
33	38.53603	-107.89557	**77**	38.74817	-108.07410			
34	38.53630	-107.88917	**78**	38.97370	-108.43369			
35	38.54128	-107.89844	**79**	38.97239	-108.43301			
36	38.54167	-107.89880	**80**	38.97352	-108.43521			
37	38.55201	-107.89333	**81**	38.96664	-108.42685			
38	38.52960	-107.97166	**82**	38.96733	-108.42753			
39	38.53041	-107.97260	**83**	38.96059	-108.42613			
40	38.53031	-107.97124	**84**	38.96338	-108.42577			

Table 2. Sample description and x-ray fluorescence analytical results.

Sample Number	Description	Elevation (ft)	Se Corr. Peak Height	Se Conc. (ppm)
1	thin crust/mixed powder	6003	162	5.5
2	pure powder w/ plant material	6058	90	3.1
3	pure powder	6053	96	3.3
4	thin crust/mixed powder	5941	3739	127.5
5	thin crust	5935	6244	212.9
6	thin crust/mixed powder	6084	667	22.7
7	mixed powder	6037	1984	67.7
8	thin crust/mixed powder	6069	420	14.3
9	thin crust/mixed powder (mainly dirt)	6104	407	13.9
10	thin crust	6103	300	10.2
11	mixed powder w/ plant material (mainly powder)	6124	906	30.9
12	pure powder	6150	143	4.9
13	pure powder	6224	49	1.7
14	mixed powder (saturated)	6205	55	1.9
15	mixed powder	6175	57	1.9
16	mixed powder/thin crusts	6159	0	0.0
17	thin crust w/ 'popcorn' appearance/mixed powder	6024	1959	66.8
18	thin crust/mixed powder	6025	315	10.7
19	mixed powder (mainly powder)/thin crust	6255	199	6.8
20	pure powder w/ plant material	6255	77	2.6
21	mixed powder/thin crust w/ plant material	6140	26	0.9
22	mixed powder	6124	42	1.4
23	nearly pure powder w/ plant material	6125	21	0.7
24	mixed powder w/ plant material (mainly powder)	6113	46	1.6
25	mixed powder w/ plant material (mainly powder)	6110	10	0.3
26	mixed powder/thin crusts	6135	89	3.0
27	mixed powder w/ plant material (mainly powder)	6135	37	1.3
28	mixed powder/thin crusts	6080	49	1.7
29	pure powder w/ plant material	6102	23	0.8
30	mixed powder/thin crusts	5642	9369	319.5
31	mixed powder (mainly salt)	5644	7785	265.5
32	mixed powder w/ plant material (mainly powder)	5644	3441	117.3

33	mixed powder/thin crusts	5645	5947	202.8
34	mixed powder/thin crusts	5671	161	5.5
35	mixed powder (mainly salt)/thin crusts	5632	2462	84.0
36	mixed powder/thin crusts	5630	12940	441.3
37	mixed powder/thin crusts	5618	87	3.0
38	mixed powder/thin crusts	5563	22	0.8
39	mixed powder/thin crusts	5575	6	0.2
40	saturated crust	5572	5	0.2
41	pure powder/thick crust w/ plant material	5585	0	0.0
42	mixed powder/small pieces of crust w/ 'popcorn' appearance	5624	0	0.0
43	mixed powder (mainly dirt)/thin crusts	5620	0	0.0
44	mixed powder (mainly dirt)/thin crusts	5619	0	0.0
45	thin crusts (mainly dirt)	5591	629	21.4
46	mixed powder w/ plant material	5427	66	2.3
47	mixed powder	5419	1	0.0
48	mixed powder (mainly salt) w/ plant material	5428	29	1.0
49	pure powder/thin crusts	5460	26	0.9
50	pure powder	5462	7	0.2
51	mixed powder (mainly salt)/thin crust	5472	21	0.7
52	pure powder	5399	17	0.6
53	mixed powder (mainly salt)	5420	158	5.4
54	mixed powder	5424	229	7.8
55	pure powder w/ plant material	5416	910	31.0
56	thick crusts (mainly salt)	5261	58	2.0
57	mixed powder/salty crusts w/ dirty plant material	5081	9	0.3
58	thick salty crusts w/ plant material	5124	3	0.1
59	pure powder	5245	0	0.0
60	pure powder	5169	0	0.0
61	mixed powder	5092	271	9.2
62	mixed powder/thin crusts	5089	188	6.4
63	thin crust in dirt matrix	4902	19	0.6
64	'popcorn' crusts (mainly dirt)	5001	44	1.5
65	pure powder	5220	419	14.3
66	mixed powder (mainly dirt)	5231	161	5.5
67	'popcorn' crusts (mainly dirt)	5318	72	2.5
68	'popcorn' crusts (mainly dirt)	5321	258	8.8
69	thin crusts in dirt matrix	5995	123	4.2
70	thin crusts	5937	74	2.5
71	mixed powder/thin crusts w/ plant material	5142	0	0.0

72	pure powder	5143	58	2.0
73	pure powder w/ 'popcorn' crusts and plant material	5151	32	1.1
74	pure powder	5147	0	0.0
75	'popcorn' crusts (mainly dirt) in mixed powder matrix	5291	26	0.9
76	thin crusts/mixed powder	4935	828	28.2
77	thin crusts/mixed powder	4934	2400	81.8
78	mixed powder/thin crusts	4715	17	0.6
79	mixed powder/thin crusts	4711	0	0.0
80	mixed powder/thin crusts	4710	41	1.4
81	mixed powder	4738	1	0.0
82	thin crust/dirt matrix	4731	5	0.2
83	dirty crust (Sample A)/pure white crust (Sample B)	4732	3	0.1
84	mixed powder/thin crusts	4741	12	0.4
85	mixed powder w/ plant material	4816	1	0.0
86	pure powder/pure crust w/ plant material	4875	29	1.0
87	mixed powder	4804	524	17.9
88	mixed powder/thin crusts	4798	3798	129.5
89	mixed powder/thin crusts	4878	65	2.2
90	powder plus some dirt	5422	1132	38.6
91	thin crust/dirt matrix	5464	7666	261.4
92	thin crust/dirt matrix	5618	476	16.2
93	mostly powder with some dirt	5134	0	0.0
94	orange crust on plant material	5134	55	1.9
95	mixed powder/thin crusts	4666	936	31.9
96	nearly pure powder with some dirt	4653	1351	46.1
97	mostly powder with some dirt	4725	2988	101.9
98	mixed powder/thin crusts	4962	1111	37.9
99	thick solid precipitate	4969	89	3.0
100	thin soil crust	4564	2216	75.6
101	mostly powder with some dirt	4563	391	13.3
102	pure powder	4611	48	1.6
103	mixed powder/thin crusts	4561	103	3.5
104	mixed powder/thin crusts	4528	124	4.2
105	thin soil crust	4534	227	7.7
106	thin soil crust	4611	21	0.7

.

Table 3. Results of sulfate mineral identification by x-ray diffraction.

Sample	Thenardit	Bloedite	Gypsum			Sample	Thenardit	Bloedite	Gypsum			Sample	Thenardit	Bloedite	Gypsum	
1	A					38	A	T				75	A	M	s	
2	A					39	A	M				76				???????
3	A					40	A	M		Mir?		77		A	s	
4	A		M			41	A	T				78	A	T		
5	A		T			42	A	T				79	A	T		
6	A		T			43	A					80	A	T		
7	A		T			44	A	M		Mir?		81	A	T		
8	A		T			45	A	T				82	T	A		
9	A		M			46	A	T				83a	A	T		
10	A		T			47	A	T				83b	A	T		
11	A		T			48	A	T				84	A	T		
12	A		T			49	A	T	t			85	A	T		
13	A	M	T	H?		50	A	T				86	A	T		
14		A				51	A	T				87	A	M		
15	A	T	T	L?		52	A		t			88	A	M	M	Hex?
16	A	M				53	A	T				89	A	T		
17	A	T	T			54	A	T				90	A			
18	A	M				55	A					90a	A	T	T	
19	A	M		H?		56	A	M				91	A	T	T	
20	A		T			57	A	M				92	A	T	T	
21	A	T	M			58	A	M				93	A	M		
22	A		T			59	A	T				94a	A	M		
23	A		T			60	A	T				94b	A	M		
24	A		T			61	A	T				95	A	T	T	
25	A		T			62	A	Y				96	A	T		
26	A	M	T	V?		63		A				97	A	M		
27	A			Mir?		64	A	M				98	A	M		
28	A	T	T			65	A					99	A	T		
29	A					66	A	M				100	A	M		
30	A		M			67	A	M		Hex?		101	A			
31	A		T			68	A	M	s	Hex?		102	A	M	M	
32	A		T			69		A				103	A	M	M	
33	A					70		A		Hex?		104a	A	T		
34	A					71	A	T				104b	A			
35	A		T			72	A					105	A			
36	A	M				73	A					106	A	M		
37	A					74	A									

A = abundant; the predominant sulfate phase. M = minor sulfate phase. T = trace amounts

Hex = Hexahydrite ($MgSO_4.6H_2O$); Mir = Mirabilite ($Na_2SO_4.10H_2O$); V = Vanthoffite ($Na_6Mg(SO_4)_4$);

L = Leowite ($Na_4Mg_2(SO_4)_4.5H_2O$)